Available online at www.sciencedirect.com
SCIENCE DIRECT®
Journal of Sound and Vibration 268 (2003) 131–147
JOURNAL OF SOUND AND VIBRATION
www.elsevier.com/locate/jsvi

Dispersion of waves and characteristic wave surfaces in functionally graded piezoelectric plates

G.R. Liu[a,*], K.Y. Dai[a], X. Han[a], T. Ohyoshi[b]

[a] *Center for Advanced Computations in Engineering Science, Department of Mechanical Engineering, National University of Singapore, 10 Kent Ridge Crescent, Singapore 119260, Singapore*
[b] *Faculty of Engineering & Resource Science, Akita University, 1-1 Tegata Gakuen-Cho Akita City 010-8502, Japan*

Received 11 February 2002; accepted 8 November 2002

Abstract

An inhomogeneous layer element method is presented to analyze the dispersion of waves and characteristic wave surfaces in plates of functionally graded piezoelectric material (FGPM). In this method, the FGPM plate is divided into a number of layered elements. The elemental elastic and electric properties are assumed as linear functions of the thickness to adopt the variety of the material property of FGPM. The Hamilton principle is applied to determine the governing equations. The phase velocity surface, phase slowness surface, phase wave surface, group velocity surface, group slowness surface, and group wave surface for FGPM plate are formulated using Rayleigh quotient and the orthogonality condition of the eigenvectors. These six surfaces are then used to illustrate the characteristics of waves in FGPM plates. Numerical examples are presented using the present formulations to analyze dispersions and characteristics of waves in FGPM plates.

1. Introduction

Materials, which respond not only to mechanical forces but also to electrical charges and generate electric potential, are named as piezoelectric materials. Piezoelectric materials are very promising which can be integrated with structural materials to form a class of "smart structures" and capable of altering the structure's response through sensing, actuation and control. To enhance the effect of piezoelectric material, a new concept of functionally graded piezoelectric material has been proposed and termed as FGPM. In the applications of FGPM to the substrate

*Corresponding author. Tel.: +65-874-6481; fax: +65-779-1459.
E-mail address: mpeliugr@nus.edu.sg (G.R. Liu).
URL: http://www.nus.edu.sg/ACES.

0022-460X/03/$ - see front matter © 2002 Elsevier Science Ltd. All rights reserved.
doi:10.1016/S0022-460X(02)01494-3

of SAW devices, the study of wave dispersion behaviors as well as wave surfaces in FGMP structures is of considerable importance.

For the characteristic analysis of waves propagating in composite plates, exact methods have been used for isotropic laminated plates [1] as well as anisotropic laminated plates [2]. Many effective numerical methods have been proposed to characterize waves in orthotropic [3,4] and other anisotropic [5,6] laminated plates. In recent years, attention has also been given to FGM structures. As the material properties of FGM change continuously, wave propagation problems related to the FGM are generally difficult to analyze. When investigating waves in an FGM plate, Liu et al. [7] have found in 1991 that Lame waves and SH waves propagate in a form of surface waves on the softer surface of FGM plates. The results show that the variation of material properties can be approximated with piecewise linear or quadratic functions of the thickness. Ohyoshi proposed an analytical method to obtain wave reflection and transmission coefficients for an FGM plate [8]. Several analytical methods have been proposed for analyzing stress waves in FGM plates [9,10]. Analytical–numerical methods were also introduced for analyzing characteristics of waves and transient responses of cylinders of functionally graded material [11,12]. For waves in laminated piezoelectric structures, matrix formulations have also been used [13,14]. Shiosaki et al. [15] have investigated Love waves in a three-layered piezoelectric structure, by using an experimental method with exact theoretical calculations. However, all of these studies dealt with homogeneous piezoelectric plates. In 1991, a hybrid numerical method was proposed and extended for FGPM and the responses of the plate excited by mechanical loads and electrodes were computed [16,17]. To the best of the authors, this is the first paper on mechanical problems for FGPM. Numerical methods for wave propagation problems for composite FGM and FGPM plates have been collected in Liu's monograph [18]. Recently, some works on free vibration problems for FGPM plates and shells were reported by Chen et al. [19,20], in which two decoupled state equations are derived with variable coefficients through the introduction of displacement and stress functions and free vibrations of functionally graded piezoceramic hollow spheres were analyzed.

In this paper, an inhomogeneous layer element method is suggested to investigate the wave characteristics of FGPM plates. In the present method, the FGPM plate is firstly divided into layered elements in the thickness direction. As the material property and electrical property do not change very sharply in the thickness direction for practical FGPM plates, the variation of the property (material and electric) within an element can be assumed as linear function in the this direction. It is also assumed that the material property is anisotropic in the plane of the plate. As the special attribute of FGPM that the material property and electric property change continuously in the thickness direction has been taken into account in each element, much less numbers of layer elements are needed to model the variation of the property. The displacement and electrostatic potential within each element are described using second order shape functions in the thickness direction. The Hamilton's principle is used to develop approximate dynamic equilibrium equations. The phase velocity surface (PVS), phase slowness surface (PSS), phase wave surface (PWS), group velocity surface (GVS), group slowness surface (GSS), and group wave surface (GWS) are formulated using the Rayleigh quotient and the orthogonality condition of the eigenvectors considering the effects of piezoelectricity. Six characteristic surfaces can be used to illustrate the characteristics of plane waves in an FGPM plate.

Numerical examples are presented for investigating the dispersion relations, group velocities, and mode shapes of harmonic plane waves propagating in a hypothetical FGPM plate. The comparisons of the characteristics of waves between the FGPM plate and those of the corresponding FGM plate are presented to investigate the piezoelectricity effect.

2. Formulation

Consider an FGPM plate with a thickness H, as shown in Fig. 1. The plate is divided into N layer elements in z direction. The thickness of the nth element is denoted by h_n. The mass density, elastic coefficient matrix, piezoelectric and dielectric material constant matrices on the lower and upper surfaces of the nth element are denoted by ρ_n^L, ρ_n^U, $\mathbf{c}_n^L = (c_{ij})_n^L$, $\mathbf{c}_n^U = (c_{ij})_n^U$ $(i,j = 1,...,6)$, $\mathbf{e}_n^L = (e_{ij})_n^L$, $\mathbf{e}_n^U = (e_{ij})_n^U$ $(i = 1,2,3;\ j = 1,...,6)$, $\mathbf{g}_n^L = (g_{ij})_n^L$, $\mathbf{g}_n^U = (g_{ij})_n^U$ $(i,j = 1,2,3)$, respectively, where the superscript "L" and "U" stand for the lower and upper surfaces, respectively. It is assumed that the material mechanical property as well as the electrical one of the nth element change linearly in the thickness direction

$$\rho_n = \rho_n^L + (\rho_n^U - \rho_n^L)\frac{z}{h_n}, \tag{1}$$

$$\mathbf{c}_n = \mathbf{c}_n^L + (\mathbf{c}_n^U - \mathbf{c}_n^L)\frac{z}{h_n}, \tag{2}$$

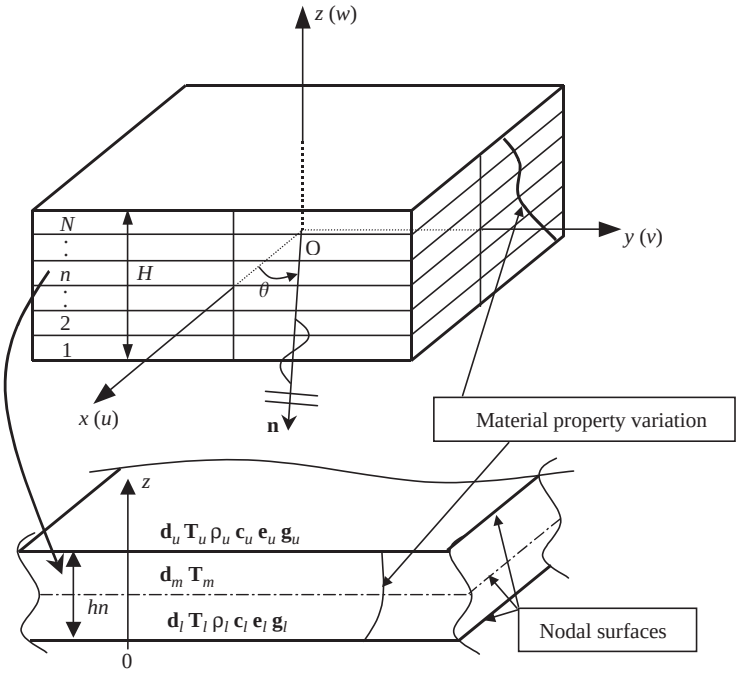

Fig. 1. An FGPM plate and the nth isolated layer element with linear variation on material property.

$$\mathbf{e}_n = \mathbf{e}_n^L + (\mathbf{e}_n^U - \mathbf{e}_n^L)\frac{z}{h_n}, \tag{3}$$

$$\mathbf{g}_n = \mathbf{g}_n^L + (\mathbf{g}_n^U - \mathbf{g}_n^L)\frac{z}{h_n}. \tag{4}$$

For FGPM plates with large property variation in the thickness direction, more elements should be used. The constitutive relations in the nth element expressing the coupling between the elastic and the electric field can be written as

$$\begin{aligned} \boldsymbol{\sigma} &= \mathbf{c}(z)\boldsymbol{\varepsilon} - \mathbf{e}^{\mathrm{T}}(z)\mathbf{E}, \\ \mathbf{D} &= \mathbf{g}(z)\mathbf{E} + \mathbf{e}(z)\boldsymbol{\varepsilon}, \end{aligned} \tag{5}$$

where ($\boldsymbol{\sigma}$, $\boldsymbol{\varepsilon}$, $\mathbf{D}$ and $\mathbf{E}$) are stress tensor, strain tensor, electric displacement vector, and electric field vector, respectively, and ($\mathbf{c}$, $\mathbf{e}$ and $\mathbf{g}$) are the elastic, piezoelectric and dielectric material matrices, accordingly. For convenience, their subscripts n's are omitted. The electrical field $\mathbf{E}$ is related to the electrical potential φ by

$$\mathbf{E} = -\mathrm{grad}\,\varphi \tag{6}$$

and the mechanical strain $\boldsymbol{\varepsilon}$ to the mechanical displacement $\mathbf{U}$ by

$$\varepsilon = \mathbf{L}_d\mathbf{U}. \tag{7}$$

The electric behavior is described by Maxwell's equation considering that the piezoelectric media are insulating

$$\mathrm{div}\,\mathbf{D} = 0. \tag{8}$$

We approximate the displacement $\mathbf{U}$ and electric static potential φ within an element as

$$\mathbf{U}(x, y, z, t) = \mathbf{N}_d(z)\mathbf{d}(x, y, t), \tag{9}$$

$$\varphi(x, y, z, t) = \mathbf{N}_\phi(z)\boldsymbol{\phi}(x, y, t), \tag{10}$$

where $\mathbf{d}$ and $\boldsymbol{\phi}$ are nodal displacement and nodal electric potential vectors

$$\begin{aligned} \mathbf{d}^{\mathrm{T}} &= \{\,\mathbf{d}_l^{\mathrm{T}} \quad \mathbf{d}_m^{\mathrm{T}} \quad \mathbf{d}_u^{\mathrm{T}}\,\}, \\ \boldsymbol{\phi}^{\mathrm{T}} &= \{\,\varphi_l^{\mathrm{T}} \quad \varphi_m^{\mathrm{T}} \quad \varphi_u^{\mathrm{T}}\,\}, \end{aligned} \tag{11}$$

in which $\mathbf{d}_i^{\mathrm{T}} = \{\,u \quad v \quad w\,\}_i$, and subscript i stands for the lower, middle or upper surface of an element. respectively.

In Eq. (9), $\mathbf{N}_d$ is the matrix of shape functions given by

$$\mathbf{N}_d = [(1 - 3\bar{z} + 2\bar{z}^2)\mathbf{I}\ 4(\bar{z} - \bar{z}^2)\mathbf{I}\ (2\bar{z}^2 - \bar{z})\mathbf{I}], \tag{12}$$

in which $\bar{z} = z/h_n$, and $\mathbf{I}$ is a 3×3 identity matrix. The vector $\mathbf{N}_\phi$ in Eq. (10) can be obtained similarly.

The governing equations of the nth element may be developed by means of Hamilton's principle

$$\delta \int L\,\mathrm{d}t = 0, \tag{13}$$

in which δ denotes the first order variation and Lagrangian term L is determined by

$$L = E_{kin} - E_{st} + E_d + W \tag{14}$$

with elastic energy E_{st}

$$E_{st} = \frac{1}{2}\int_0^{h_n} \varepsilon^{\mathrm{T}}\boldsymbol{\sigma}\,\mathrm{d}z \tag{15}$$

and dielectric energy E_d

$$E_d = \frac{1}{2}\int_0^{h_n} \mathbf{E}^{\mathrm{T}}\mathbf{D}\,\mathrm{d}z \tag{16}$$

and kinetic energy E_{kin}

$$E_{kin} = \frac{1}{2}\int_0^{h_n} \rho_n \ddot{\mathbf{U}}^{\mathrm{T}}\ddot{\mathbf{U}}\,\mathrm{d}z \tag{17}$$

where the superscript T denotes the transposed matrix. W is generated by external mechanical or electrical excitation with the form of

$$W = \mathbf{d}^{\mathrm{T}}\mathbf{F} + \boldsymbol{\phi}^{\mathrm{T}}\mathbf{Q}_z, \tag{18}$$

where $\mathbf{F}$ is a nodal external force vector, and $\mathbf{Q}_z$ is a nodal charge vector in the z direction.

Substituting Eqs. (15)–(18) into Eqs. (14), (13) with the application of Eqs. (1)–(10), we obtain a set of differential equations with respect to x, y and t for the nth element

$$\mathbf{T}_n = \mathbf{M}_n\ddot{\boldsymbol{\xi}}_n + \mathbf{K}_{Dn}\boldsymbol{\xi}_n. \tag{19}$$

Assembling the matrices of all the elements, the system differential equation for the whole FGPM plate can be obtained which is similar to Eq. (19) except that all the subscripts "n" are replaced by "t". Here "t" indicates the matrices correspond to the whole FGPM plate, the matrices $\mathbf{K}_{Dt}$, $\mathbf{M}_t$, $\mathbf{T}_t$ and $\boldsymbol{\xi}_t$ can be obtained by assembling the corresponding matrices of adjacent elements. The detailed formulations can be referred in literature [17,18,21].

3. Analysis

3.1. Equations in transform domain

We introduce the Fourier transformations with respect to the horizontal co-ordinates x and y as follows:

$$\tilde{\boldsymbol{\xi}}_t(k_x, k_y, t) = \int_{-\infty}^{\infty}\int_{-\infty}^{\infty} \boldsymbol{\xi}_t(x, y, t)\mathrm{e}^{-\mathrm{i}k_x x}\mathrm{e}^{-\mathrm{i}k_y y}\,\mathrm{d}x\,\mathrm{d}y, \tag{20}$$

where $\mathrm{i} = \sqrt{-1}$, k_x and k_y are the wave numbers for wave propagation in the x- and y-axis, respectively. The application of Fourier transformations by Eq. (20) to system equations leads to the following governing equation in wave number domain:

$$\tilde{\mathbf{T}}_t = \mathbf{M}_t\ddot{\tilde{\boldsymbol{\xi}}}_t + \mathbf{K}_t\tilde{\boldsymbol{\xi}}_t. \tag{21}$$

In this equation, $\tilde{\mathbf{T}}_t$, $\ddot{\tilde{\boldsymbol{\xi}}}_t$ and $\tilde{\boldsymbol{\xi}}_t$ are the transformations of $\mathbf{T}_t$, $\ddot{\boldsymbol{\xi}}_t$ and $\boldsymbol{\xi}_t$, respectively, and $\mathbf{K}_t$ is given by

$$\mathbf{K}_t = \begin{bmatrix} \mathbf{A}_t & \mathbf{C}_t \\ \mathbf{C}_t^{\mathrm{T}} & \mathbf{G}_t \end{bmatrix}, \tag{22}$$

where $\mathbf{A}_t$ is the mechanical stiffness matrix given by

$$\mathbf{A}_t = k_x^2\mathbf{A}_{1t} + k_xk_y\mathbf{A}_{2t} + k_y^2\mathbf{A}_{3t} + \mathrm{i}k_x\mathbf{A}_{4t} + \mathrm{i}k_y\mathbf{A}_{5t} + \mathbf{A}_{6t}. \tag{23}$$

The piezoelectric coupling matrix, $\mathbf{C}_t$, and dielectric stiffness matrix, $\mathbf{G}_t$, are of the same form as Eq. (23), with $\mathbf{A}$ replaced by $\mathbf{C}$ and $\mathbf{G}$, respectively.

3.2. PVS and PSS

Under the action of harmonic force, $\tilde{\boldsymbol{\xi}}_t$ is also in harmonic form of

$$\tilde{\boldsymbol{\xi}}_t = \tilde{\boldsymbol{\xi}}_t(k_x, k_y)\exp(-\mathrm{i}\omega t). \tag{24}$$

When no external forces $\mathbf{F}_t$ or charges $\mathbf{Q}_{zt}$ are applied to the plate, we obtain the following eigenvalue problem after the substitution of the above equation into Eq. (21):

$$\mathbf{K}_t\tilde{\boldsymbol{\xi}}_t - \omega^2\mathbf{M}_t\tilde{\boldsymbol{\xi}}_t = \mathbf{O}, \tag{25}$$

where ω is the angular frequency and $\mathbf{O}$ is a zero vector. For a plane wave propagating in the direction of θ, we have

$$k_x = k\cos\theta, \quad k_y = k\sin\theta, \tag{26}$$

where k is the wave number of the plane wave.

The mth eigenvalues and eigenvectors of Eq. (25) can be written in the form of the well-known Reyleigh quotient

$$\omega_m^2 = \frac{\tilde{\boldsymbol{\psi}}_m^L\mathbf{K}_t\tilde{\boldsymbol{\psi}}_m^R}{\tilde{\boldsymbol{\psi}}_m^L\mathbf{M}_t\tilde{\boldsymbol{\psi}}_m^R}, \tag{27}$$

$$\tilde{\boldsymbol{\psi}}_m^L = \{\boldsymbol{\Lambda}_m^L\ \boldsymbol{\phi}_m^L\}, \quad (\tilde{\boldsymbol{\psi}}_m^R)^{\mathrm{T}} = \{(\boldsymbol{\Lambda}_m^R)^{\mathrm{T}}\ (\boldsymbol{\phi}_m^R)^{\mathrm{T}}\}, \tag{28}$$

where superscripts "L" and "R" stand for the left and right eigenvectors, and $\boldsymbol{\Lambda}_m$ and $\boldsymbol{\phi}_m$ are the mth displacement and electropotential eigenvectors, respectively.

Applying the reduction technique with the help of Eqs. (21) and (22), Eq. (25) can be changed into

$$\mathbf{K}_{st}\tilde{\mathbf{d}}_t - \omega^2\mathbf{M}_{st}\tilde{\mathbf{d}}_t = \mathbf{O}, \tag{29}$$

$$\mathbf{K}_{st} = \mathbf{A}_t + \mathbf{C}_t\mathbf{G}_t^{-1}\mathbf{C}_t^{\mathrm{T}}. \tag{30}$$

From the solutions of the above two equations, we can get ω_m, $\boldsymbol{\Lambda}_m$ and then $\boldsymbol{\phi}_m$ can also be obtained from

$$\boldsymbol{\phi}_m = \mathbf{G}_t^{-1}\mathbf{C}_t^{\mathrm{T}}\boldsymbol{\Lambda}_m. \tag{31}$$

The phase velocity of the mth mode is defined as

$$c_m(\theta) = \omega_m(\theta)/k \tag{32}$$

and the phase slowness s_m is the reciprocal of the phase velocity c_m. When wave propagation angle θ changes from 0 to 2π, we can plot the PVS and thereafter the PSS.

3.3. Phase wave surface

PWS of the mth mode is found by calculating the envelope formed by straight lines of plane wave fronts. PWS for anisotropic laminated plates without piezoelectricity is given by Liu and Tani, et al. [22]. PWS can be drawn in the polar co-ordinate $(|\mathbf{r}_m|, \beta_P)$, where

$$|\mathbf{r}_m| = c_m\sqrt{1+\alpha_s^2}, \quad \beta_P = \tan^{-1}\alpha_s + \theta, \tag{33}$$

$$\alpha_s = \frac{\tilde{\boldsymbol{\psi}}_m^L \mathbf{K}_{t,\theta} \tilde{\boldsymbol{\psi}}_m^R}{2\tilde{\boldsymbol{\psi}}_m^L \mathbf{K}_t \tilde{\boldsymbol{\psi}}_m^L}, \tag{34}$$

$$\mathbf{K}_{t,\theta} = \frac{\partial \mathbf{K}_t}{\partial\theta} = \begin{bmatrix} \mathbf{A}_{t,\theta} & \mathbf{C}_{t,\theta} \\ \mathbf{C}_{t,\theta}^{\mathrm{T}} & -\mathbf{G}_{t,\theta} \end{bmatrix}, \tag{35}$$

$$\begin{aligned} \mathbf{A}_{t,\theta} = \frac{\partial \mathbf{A}_t}{\partial\theta} = & -\mathbf{A}_{1t}k^2 \sin 2\theta + \mathbf{A}_{2t}k^2 \cos 2\theta. \\ & + \mathbf{A}_{3t}k^2 \sin 2\theta - \mathrm{i}\mathbf{A}_{4t}k \sin\theta + \mathrm{i}\mathbf{A}_{5t}k\cos\theta, \end{aligned} \tag{36}$$

$\mathbf{C}_{t,\theta}$ and $\mathbf{G}_{t,\theta}$ can be deduced in the same way.

3.4. GVS and GSS

GVS shows the dependence of the energy propagation velocity of a plane wave on the direction of propagation θ. Using its definition and Eq. (27), we obtain the group velocity for the mth mode of the plane wave as

$$c_{gm} = \frac{\mathrm{d}\omega}{\mathrm{d}k} = \frac{\tilde{\boldsymbol{\psi}}_m^L \mathbf{K}_{t,k} \tilde{\boldsymbol{\psi}}_m^R}{2\omega_m \tilde{\boldsymbol{\psi}}_m^L \mathbf{M}_t \tilde{\boldsymbol{\psi}}_m^R}, \tag{37}$$

where

$$\mathbf{K}_{t,k} = \frac{\partial \mathbf{K}_t}{\partial k} = \begin{bmatrix} \mathbf{A}_{t,k} & \mathbf{C}_{t,k} \\ \mathbf{C}_{t,k}^{\mathrm{T}} & -\mathbf{G}_{t,k} \end{bmatrix}, \tag{38}$$

$$\begin{aligned} \mathbf{A}_{t,k} = \frac{\partial \mathbf{A}_t}{\partial k} = & 2k\mathbf{A}_{1t}\cos^2\theta + 2k\mathbf{A}_{2t}\cos\theta\sin\theta \\ & + 2k\mathbf{A}_{3t}\sin^2\theta + \mathrm{i}\mathbf{A}_{4t}\cos\theta + \mathrm{i}\mathbf{A}_{5t}\sin\theta. \end{aligned} \tag{39}$$

Similarly, $\mathbf{C}_{t,k}$ and $\mathbf{G}_{t,k}$ can be obtained from Eq. (23) in the same way. The group slowness for the mth mode is the reciprocal of the group velocity. The GSS shows the dependence of the relative arrival time of the energy of a plane wave on the direction of wave propagation.

3.5. Group wave surface

GWS shows the envelope of group propagation front. It also can be drawn in the polar coordinate ($|\mathbf{R}_m|$, β_G), where

$$|\mathbf{R}_m| = c_{gm}\sqrt{1+\alpha_q^2}, \quad \beta_G = \tan^{-1}\alpha_q + \theta, \tag{40}$$

$$\alpha_q = \frac{\tilde{\boldsymbol{\psi}}_m^L \mathbf{K}_{t,k\theta}\tilde{\boldsymbol{\psi}}_m^R - \tilde{\boldsymbol{\psi}}_m^L \mathbf{K}_{t,\theta}\tilde{\boldsymbol{\psi}}_m^R c_{gm}/\omega_m}{\tilde{\boldsymbol{\psi}}_m^L \mathbf{K}_{t,k}\tilde{\boldsymbol{\psi}}_m^R}, \tag{41}$$

where

$$\mathbf{K}_{t,k\theta} = \frac{\partial^2 \mathbf{K}_t}{\partial k \partial \theta} = \begin{bmatrix} \mathbf{A}_{t,k\theta} & \mathbf{C}_{t,k\theta} \\ \mathbf{C}_{t,k\theta}^{\mathrm{T}} & -\mathbf{G}_{t,k\theta} \end{bmatrix}, \tag{42}$$

$$\begin{aligned} \mathbf{A}_{t.k\theta} = \frac{\partial^2 \mathbf{A}_t}{\partial k \partial \theta} = & -2\mathbf{A}_{1t}k\sin 2\theta + 2\mathbf{A}_{2t}k\cos 2\theta \\ & + 2\mathbf{A}_{3t}k\sin 2\theta - \mathrm{i}\mathbf{A}_{4t}\sin\theta + \mathrm{i}\mathbf{A}_{5t}\cos\theta. \end{aligned} \tag{43}$$

$\mathbf{C}_{t,k\theta}$ and $\mathbf{G}_{t,k\theta}$ are in the same form as Eq. (43) with $\mathbf{A}$ replaced by $\mathbf{C}$ and $\mathbf{G}$, respectively.

Table 1
Natural frequencies of the lowest six modes for the FGPM and FGM plate ($\theta = 0$)

$\bar{k}$	Plate	M1	M2	M3	M4	M5	M6
3.436	FGPM	4.4809	5.4231	7.2377	7.9438	8.2469	11.495
		(0.36%)	(0.43%)	(0.21%)	(0.23%)	(0.21%)	(0.03%)
	FGM	4.4648	5.3999	7.2224	7.9254	8.2299	11.492
16.20	FGPM	16.637	18.634	22.968	23.677	27.228	28.348
		(1.18%)	(2.54%)	(0.56%)	(0.88%)	(1.5%)	(0.25%)
	FGM	16.443	18.173	22.840	23.469	26.820	28.272

Table 2
Dimensionless group velocities of the lowest six modes for the FGPM and FGM plate ($\theta = 0$)

$\bar{k}$	Plate	M1	M2	M3	M4	M5	M6
3.436	FGPM	1.7377	1.1124	1.1202	0.78056	1.6809	1.7911
		(0.15%)	(0.55%)	(0.72%)	(3.2%)	(0.31%)	(0.06%)
	FGM	1.7351	1.1063	1.1283	0.75660	1.6757	1.7900
16.20	FGPM	0.87358	1.0418	1.0907	1.1213	1.2440	1.1379
		(2.4%)	(3.7%)	(0.13%)	(5.9%)	(0.80%)	(1.1%)
	FGM	0.85284	1.0050	1.0921	1.0586	1.2341	1.1252

Up to now, the six characteristic wave surfaces have been formulated considering the piezoelectric effect of an FGPM plate.

4. Numerical results and discussions

Based on the foregoing formulations, a FORTRAN 90 program has been developed. In this section, numerical results are presented to illustrate the piezoelectric effect on the dispersion and characteristics of waves, the displacement mode shapes, as well as the electric potential distribution of a hypothetical FGPM plate.

The material properties on the upper surface ($z = H$) of the hypothetical FGPM plate are the same as those of the homogeneous $z - x$ $LiTaO_3$ plate (see Ref. [23] for material constants), i.e.,

$$\mathbf{c}^U = \mathbf{c}, \quad \mathbf{e}^U = \mathbf{e}, \quad \mathbf{g}^U = \mathbf{g}, \quad \rho^U = \rho, \tag{44}$$

where $\mathbf{c}$, $\mathbf{e}$ and $\mathbf{g}$ are the elastic, piezoelectric and dielectric constant matrices of $z - x$ $LiTaO_3$ plate, respectively. The material properties on the lower surface of the plate ($z = 0$) are assumed to be

$$\mathbf{c}^L = 12\mathbf{c}, \quad \mathbf{e}^L = 0.1\mathbf{e}, \quad \mathbf{g}^L = 0.5\mathbf{g}, \quad \rho^L = 1.8\rho. \tag{45}$$

In the thickness direction, the elastic constants are assumed to vary as the following function:

$$\mathbf{c}(z) = \mathbf{c}^U + (\mathbf{c}^L - \mathbf{c}^U)(1 - z/H)^2 \tag{46}$$

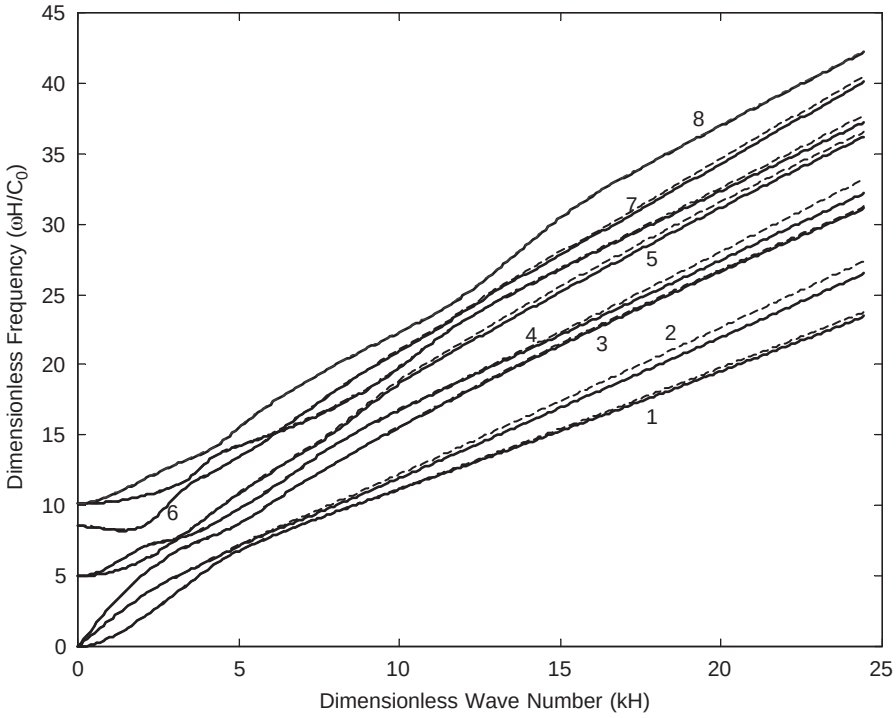

Fig. 2. Frequency spectra of the lowest eight modes for an FGM plate (solid line) and an FGPM plate (dashed line) ($\theta = 0.0$).

and the same function is applied to $\mathbf{e}(z)$, $\mathbf{g}(z)$ and $\rho(z)$, respectively. For convenience, we introduced the following non-dimensional parameters in the following calculation:

$$\bar{x} = x/H, \quad \bar{z} = z/H, \quad \bar{k} = k_x H, \quad \bar{c}_g = c_g/c_0, \quad c_0 = \sqrt{c_{66}^0/\rho_0}, \tag{47}$$

where ρ_0 is the mass density and c_{66}^0 is the elastic constant c_{66} of the z–x $LiTaO_3$ plate [23].

In order to investigate the piezoelectricity effect, we consider a corresponding FGM plate whose material property is the same as the FGMP mentioned above but without piezoelectricity.

Firstly we investigate the piezoelectricity effect. The natural frequencies and group velocities are calculated and listed in Tables 1 and 2, respectively. The comparisons of the natural frequencies and group velocities between the FGPM plate and the corresponding FGM plate are also presented in these tables. Our calculations indicate that the effect of piezoelectricity changes the natural frequencies and group velocities less than 2% and 3% on the average, respectively, compared with FGM plate.

The frequency spectra of the lowest eight modes are plotted in Fig. 2 when wave propagates in x-axis direction. The comparison of the frequency spectra between the FGPM and FGM plate is also illustrated in this figure. It can be seen that the frequency increases when wave number or the order of mode becomes larger. For a definite mode, the piezoelectric effect becomes stronger as wave number increases. The phase velocities will stop decreasing when wave number becomes large enough and their final values range from 1.0 to 2.0 for the lowest eight modes. Fig. 3 gives

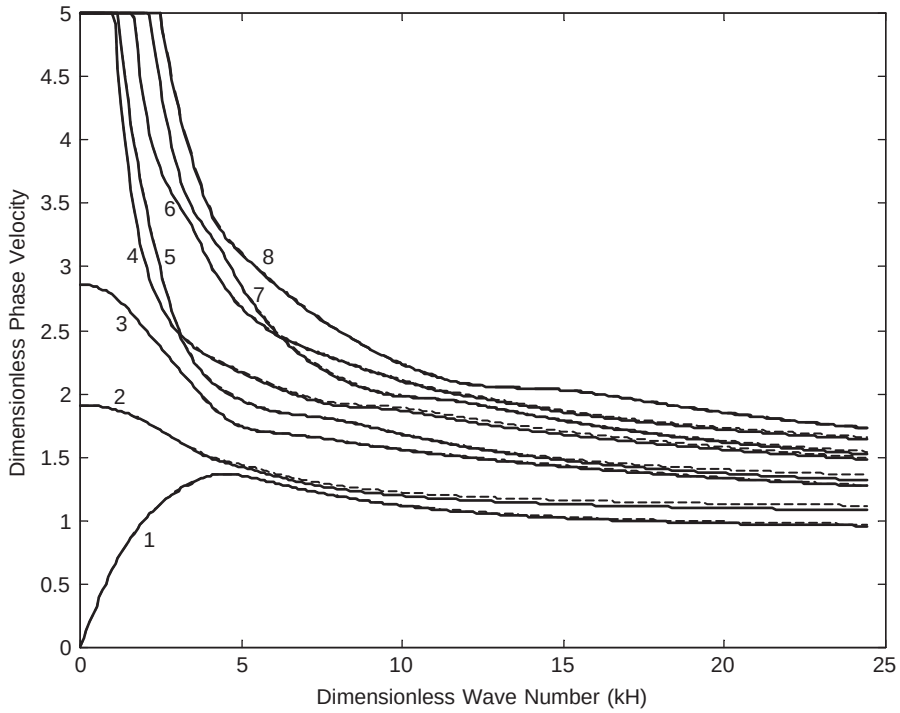

Fig. 3. Phase velocity spectra of the lowest eight modes for an FGM plate (solid line) and an FGPM plate (dashed line) ($\theta = 0.0$).

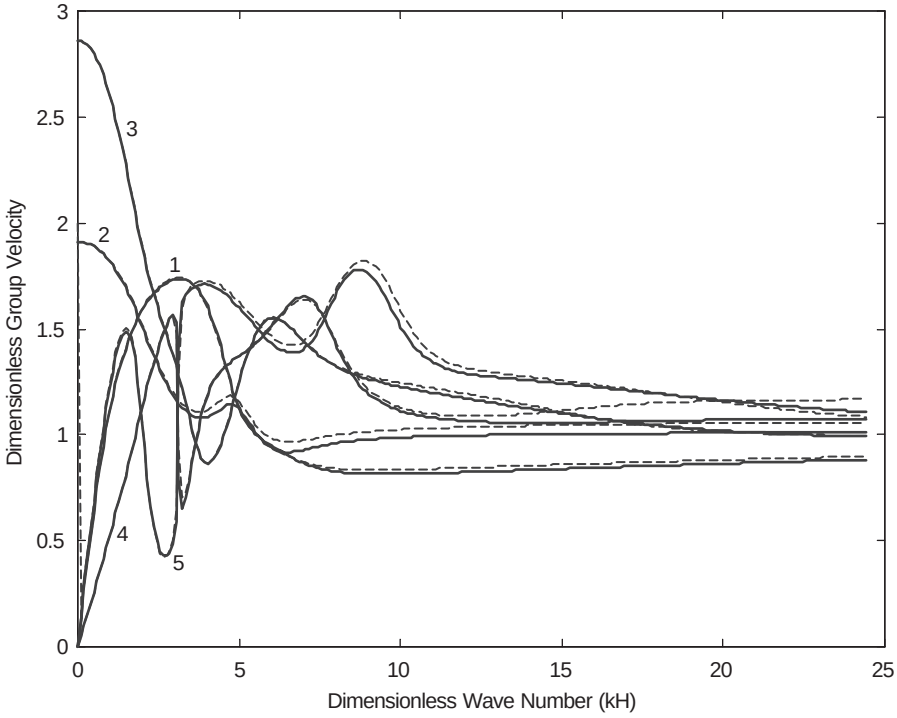

Fig. 4. Group velocity spectra of the lowest five modes for an FGM plate (solid line) and an FGPM plate (dashed line) ($\theta = 0.0$).

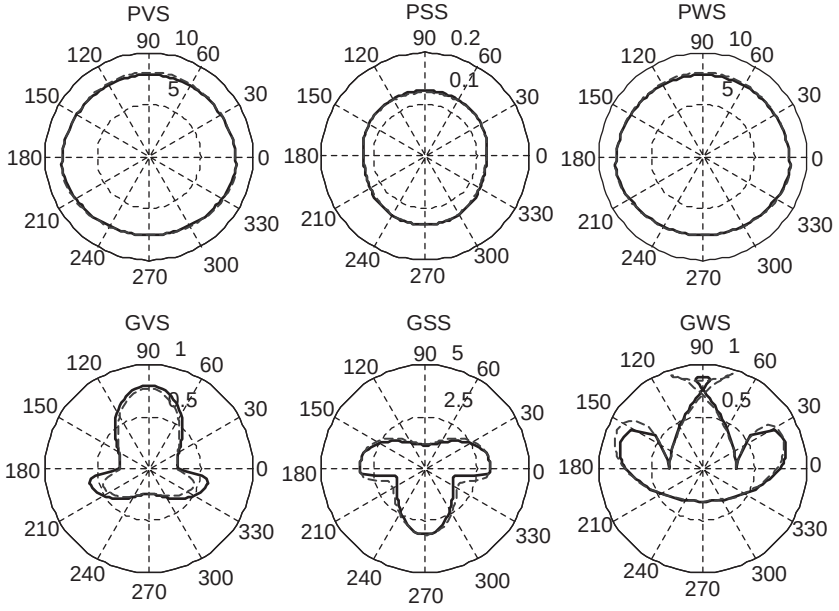

Fig. 5. The characteristic surface for an FGM plate (solid line) and an FGPM plate (dashed line) ($\bar{k} = 5.007$, fourth mode).

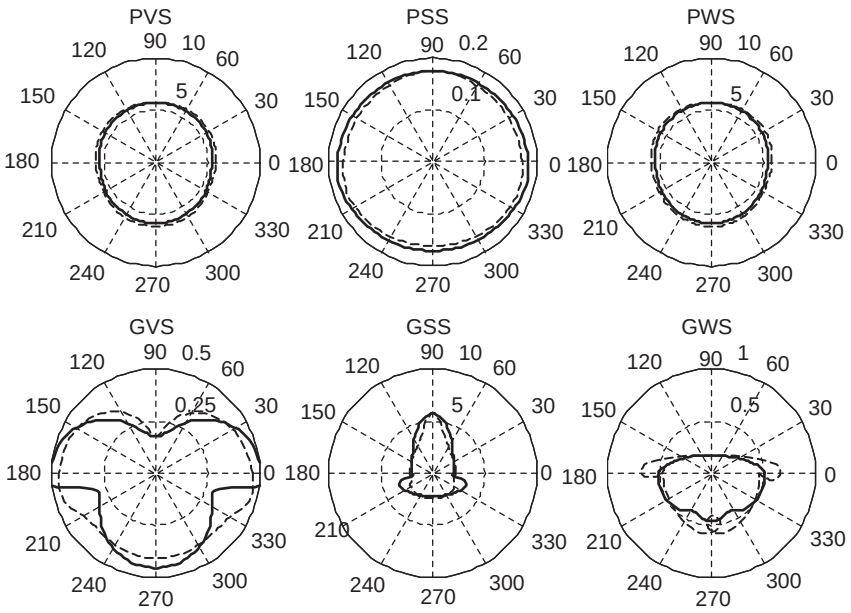

Fig. 6. The characteristic surface for an FGM plate (solid line) and an FGPM plate (dashed line) ($\bar{k} = 5.007$, fifth mode).

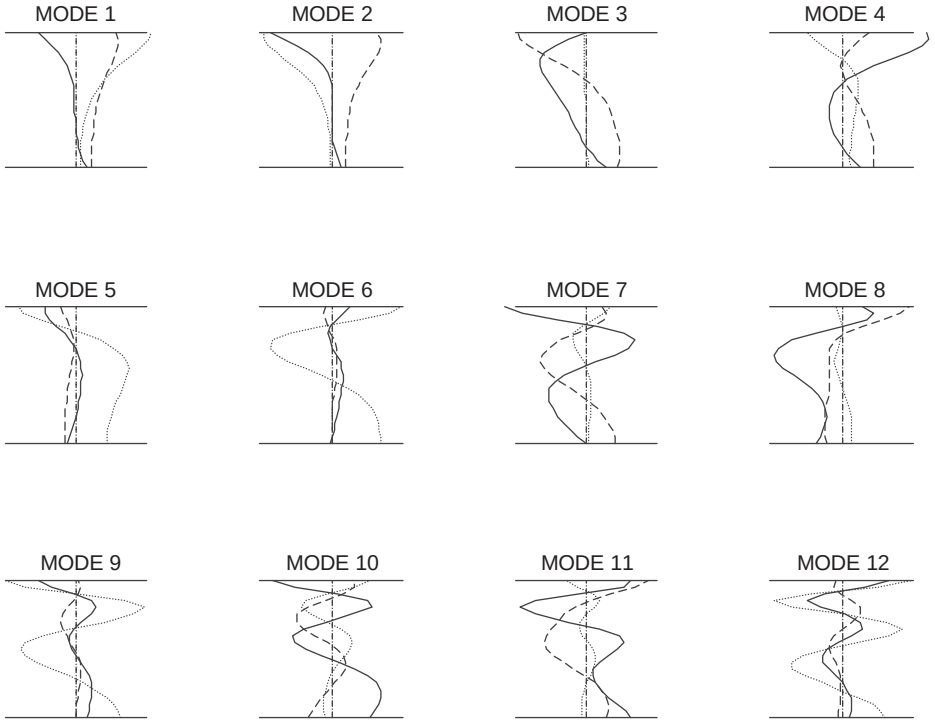

Fig. 7. Displacement distribution in the thickness direction of an FGPM plate ($\bar{k} = 5.007$, $\theta = 0$, solid line: u, dotted line: v, dashed line: w).

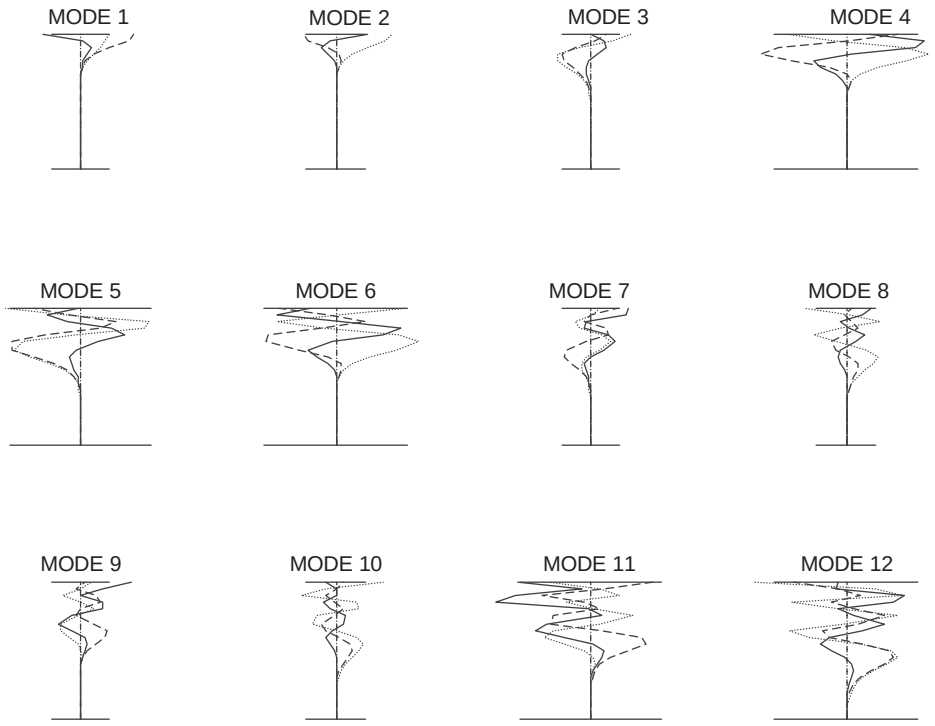

Fig. 8. Displacement distribution in the thickness direction of an FGPM plate ($\bar{k} = 30.042$, $\theta = 0$, solid line: u, dotted line: v, dashed line: w).

comparison of the phase velocity spectra of the lowest eight modes between the FGPM and FGM plate. The similar phenomena as Fig. 2 can be observed. Fig. 4 shows the group velocity spectra of the lowest five modes of FGM and FGPM plates. It is shown that the smaller the wave number, the more sharply the group velocity curves oscillate. Similar to the phase velocities, group velocity curves will get almost unchangeable within the range 1.0–1.5 for the lowest eight modes when wave number gets large enough. The group velocities are generally smaller than the corresponding phase velocities. In our computations, group velocities are observed in a smaller wave number range for the seventh and eight mode for this case. This means that the energy propagates in the opposite direction to that of the phase propagation. From these figures the dispersion behaviors have been clearly demonstrated for functionally graded piezoelectric plate. Comparing the curves for FGM and FGPM plate in Figs. 2–4, we can see that the piezoelectric effect is small, less than 5% on average. However, the effects become significant for large wave number or small wavelength. Therefore, in micro-scale SAW devices, the operating frequency is usually very high and the wavelength is very small, the piezoelectric effects will be prominent.

The piezoelectricity effect on wave surfaces is also investigated. The characteristic surfaces of the fourth and fifth mode are selected and plotted in Figs. 5 and 6, respectively. Both the FGPM plate and the corresponding FGM plate are presented together. Comparing the characteristic

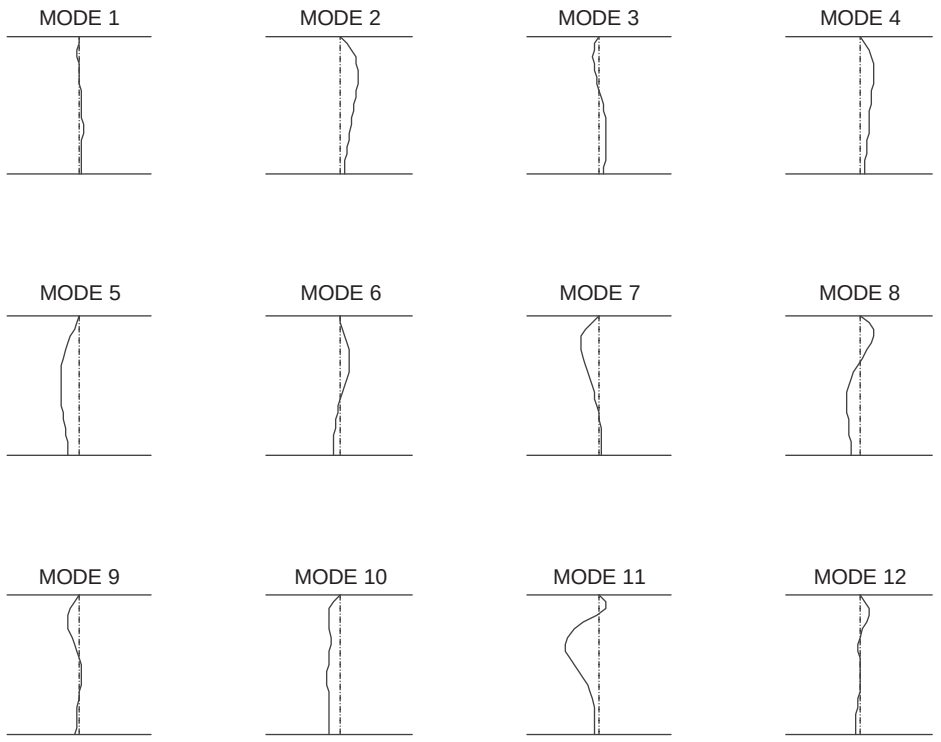

Fig. 9. Electric potential distribution in the thickness direction of an FGPM plate ($\bar{k}=5.007$, $\theta=0$).

surfaces of the first several lower modes, we notice that, all the PVS, PSS and PWS are similar to irregular eclipses while GVS, GSS and GWS changes significantly in shapes and are also different from mode to mode accordingly. All the six surfaces have only one symmetric axis. All the piezoelectrically stiffened and unstiffened wave surfaces are direction dependent. From these figures, it can be seen that PVS, PSS and PWS are generally in considerable difference from GVS, GSS and GWS for all modes due to the strong dispersion. Comparing PVS and GVS, we can conclude that the direction in which the plane wave propagates fastest is different from that of the fastest energy propagation. However, it is still possible in piezoelectric plate that the energy propagation concentrates in the same directions since many modes propagate with the same group velocity in those directions. Note that, although the above comments are derived from modes 4 and 5, they are also applicable to other lower modes not plotted here.

The displacement mode shapes and the electric potential distribution of the FGPM plate are also investigated. Figs. 7 and 8 show the lowest 12 displacement mode shapes of the FGPM plate for $\bar{k}=5.007$ and 30.042. It can be seen that the displacements in FGPM plate decay with distance from the upper to lower surface, especially for the lowest modes. As the wave number increases, they will decay more significantly from the upper surface. Figs. 9 and 10 give the corresponding electrostatic potential modes for $\bar{k}=5.007$ and 30.042, respectively. The similar phenomenon as illustrated in Figs. 7 and 8 occurs in these two figures.

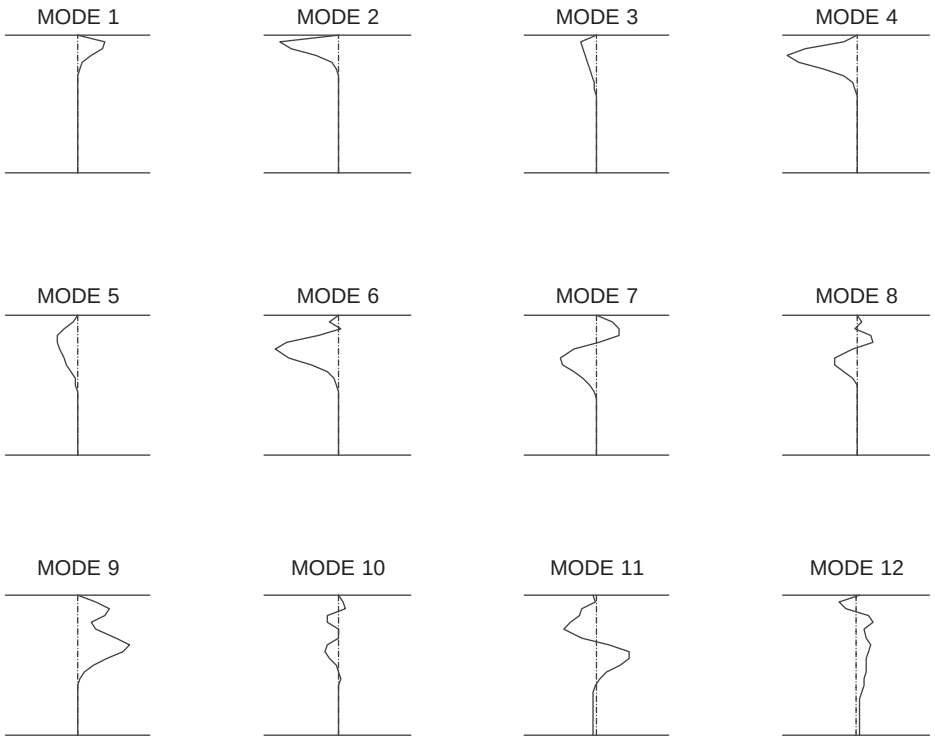

Fig. 10. Electric potential distribution in the thickness direction of an FGPM plate ($\bar{k}=30.042$, $\theta=0$).

5. Conclusions

The dispersion behaviors and characteristics of wave in functionally graded piezoelectric plates are investigated. Piezoelectricity effects on the dispersion and characteristics of waves are provided by comparison between the FGPM plate and the corresponding FGM plate. With the six wave surfaces, the characteristics of the dispersive and anisotropic waves in graded piezoelectric plates can be clearly revealed. The displacements decay with distance from softer surface to the harder surface of FGPM plates. The larger the wave number, the stronger the confinement of the displacements to the softer surface. The penetration depth of surface waves in FGPM plates can therefore be controlled by adjusting the gradient of the material properties.

Appendix A. Nomenclature

c	matrix of elastic constants
c_m	phase velocity
c_{gm}	group velocity
d	nodal displacement vector
$\tilde{\mathbf{d}}$	Fourier transformation of nodal displacement vector
D	electric displacement vector

e	piezoelectric matrix
E	electric field vector
E_d	dielectric energy
E_{kin}	kinetic energy
E_{st}	elastic energy
F	external force vector
$\tilde{\mathbf{F}}$	Fourier transformation of external force vector
H	thickness of the plate
h_n	thickness of the nth layer element
$\mathrm{i} = \sqrt{-1}$	imaginary unit
I	3×3 identity matrix
K	stiffness matrix
k	wave number
M	mass matrix
N	shape function matrix
s_m	phase slowness
t	time
T	general force vector
u, v, w	displacement components
x, y, z	Cartesian co-ordinates
$\boldsymbol{\sigma}$	vector of stresses
$\boldsymbol{\varepsilon}$	vector of strains
$\tilde{\boldsymbol{\psi}}$	eigenvector
$\boldsymbol{\xi}$	general displacement vector
$\tilde{\boldsymbol{\xi}}$	Fourier transformation of general displacement vector
ω	angular frequency

Superscripts

D	additional matrix due to the variation of material properties in thickness
l	matrices for homogeneous element constants at its lower surface
L, U	lower, and upper nodal surface of a layer element for plate, respectively
R, L	right and left eigenvectors
T	transposed matrix

Subscripts

l, m, u	lower, middle and upper surface of a layer element for plate, respectively
t	variables related to the total structure
$1, 2, \cdots, n$	number of layer elements

References

[1] W. Tompson, Transmission of elastic waves through a stratified medium, Journal of Applied Physics 21 (1950) 89–93.

[2] G.R. Liu, J. Tani, K. Watanabe, T. Ohyoshi, Lamb wave propagation in anisotropic laminates, American Society of Mechanical Engineers Journal of Applied Mechanics 57 (1990) 923–929.
[3] S.B. Dong, R.B. Nelson, On natural vibrations and waves in laminated orthotropic plates, American Society of Mechanical Engineers Journal of Applied Mechanics 39 (1972) 739–745.
[4] R.B. Nelson, S.B. Dong, R.D. Kalra, Vibrations and waves in laminated orthortropic circular cylinders, Journal of Sound and Vibration 18 (1971) 429–444.
[5] E. Kausel, Wave propagation in anisotropic layered media, International Journal for Numerical Methods in Engineering 23 (1986) 1567–1578.
[6] E. Adler, Matrix methods applied to acoustic waves in multilayers, IEEE Transactions on Ultrasonics, Ferroelectrics, and Frequency Control 37 (6) (1990) 485–490.
[7] G.R. Liu, J. Tani, T. Ohyoshi, Lamb waves in a functionally gradient material plates and its transient response,: Part 1: Theory, Part 2: Calculation results, Transactions of the Japan Society of Mechanical Engineers 57(A) (535) (1991) 603–611.
[8] T. Ohyoshi, Linearly inhomogeneous layer element for reflectance evaluation of inhomogeneous layers, Dynamic Response Behavior Composition 46 (1995) 121–126.
[9] G.R. Liu, X. Han, K.Y. Lam, Stress waves in functionally gradient materials and its use for material characterization, Composites Part B 30 (1999) 383–394.
[10] X. Han, G.R. Liu, K.Y. Lam, T. Ohyoshi, A quadratic layer element for analyzing stress waves in functionally graded materials and its applications for material characterization, Journal of Sound and Vibration 236 (2) (2000) 307–321.
[11] X. Han, G.R. Liu, Z.C. Xi, K.Y. Lam, Characteristic of waves in a functionally graded cylinder, International Journal for Numerical Methods in Engineering 53 (2002) 653–676.
[12] X. Han, G.R. Liu, Z.C. Xi, K.Y. Lam, Transient waves in a functionally graded cylinder, International Journal of Solids and Structures 38 (2001) 3021–3037.
[13] A.M.B. Braga, G. Herrmann, in: A.K. Mal, T.C.T. Ting (Eds.), Plane Waves in Anisotropic Layered Composites, Vol. 90, ASME-AMD, New York, 1988, pp. 81–98.
[14] E. Adler, Bulk and surface acoustic waves in anisotropic solids, International Journal on High Speed Electronics and Systems 10 (3) (2000) 648–653.
[15] T. Shiosai, Y. Mikamura, F. Takeda, A. Kawabata, High-coupling and high-velocity SAW using ZnO and AlN Films on a glass substrate, IEEE Transactions on UFFC 33-3 (1986) 324–330.
[16] G.R. Liu, J. Tani, Characteristics of wave propagation in functionally gradient piezoelectric material plates and its response analysis: Part 1: theory, Part 2: calculation results, Transactions of the Japan Society of Mechanical Engineers Japan 57(A) (541) (1991) 2122–2133.
[17] G.R. Liu, J. Tani, Surface waves in functionally gradient piezoelectric plates, Transactions of the American Society of Mechanical Engineers 116 (1994) 440–448.
[18] G.R. Liu, Z.C. Xi, Elastic Waves in Anisotropic Laminates, CRC Press, New York, 2001.
[19] W.Q. Chen, L.Z. Wang, Y. Lu, Free vibrations of functionally graded piezoceramic hollow spheres with radial polarization, Journal of Sound and Vibration 251 (1) (2002) 103–114.
[20] W.Q. Chen, H.J. Ding, On free vibration of a functionally graded piezoelectric rectangular plate, Acta Mechanica 153 (2002) 207–216.
[21] G.R. Liu, J. Tani, T. Ohyoshi, in: Masao Yamanouchi, et al. (Eds.), Lame wave propagation in anisotropic functionally gradient materials, Proceedings of the First International Symposium on Functionally Gradient Materials, Sendai: Functionally Gradient Materials Forum, 1990, pp. 59–64.
[22] G.R. Liu, J. Tani, T. Ohyoshi, K. Watanabe, Characteristic wave surfaces in anisotropic laminated plates, Journal of Vibration and Acoustics 113 (1991) 279–285.
[23] G.G. John, A.K. John, B. Arthur, Piezoelectric materials for acoustic wave applications, IEEE Transactions on Ultrasonics, Ferroelectrics, and Frequency Control 41 (1) (1994) 53–59.